EUROPEAN ORGANIZATION FOR NUCLEAR RESEARCH

LHCb 2000-077 RICH
September 1, 2000

# The mechanical design of RICH-1

G.J. Barber[2)], N.H. Brook[1)], A. Duane[2)], R.D. Head[1)], J.A. Lidbury[3)], P. Savage[2)], D.M. Websdale[2)],

**Abstract**

We describe the current design of RICH-1, the constraints imposed by its position in the LHCb experiment and the optimisation of the critical parameters.

[1)] University of Bristol
[2)] Imperial College, London
[3)] Rutherford-Appleton Laboratory, Chilton

## 1 Introduction

This note is intended to provide background information for the RICH TDR. It describes the current design of the RICH-1 mechanics and records the decisions made in reaching it.

## 2 Physics performance required

RICH-1 is required to cover the solid angle accepted by the spectrometer. For small angles, the beam-pipe limits this to 25mrad. For large angles, the magnetic shield plate and the magnet yoke limit the solid angle to $\pm 300$ mrad (horizontally) $\times$ $\pm 250$ mrad (vertically).

The requirements on velocity resolution are described in the Technical Proposal; see ref[1] chapter 9. RICH-1 and RICH-2 together must distinguish K from $\pi$ mesons with momenta between 1 and 150 Gev/$c$. RICH-2 takes over from RICH-1 for momenta between 16 and 60 Gev/$c$, but with reduced angular acceptance.

RICH-1 should not interfere with other LHCb detectors. The electromagnetic calorimeter could be affected if electrons radiate a significant fraction of their energy or if a significant fraction of photons convert. Tracking of charged particles should not be spoiled by too much scattering. The minimum possible amount of material would be that of the radiators: 5.9% $X_0$ in the present design.

## 3 Additional features required

It has emerged since the TP that some of the support needed by the beam-pipe should be provided by RICH-1. The beam-pipe will need to be baked out, about once a year, at a temperature of up to 250°C. If the piece of beam-pipe passing through RICH-1 fails, it should be possible to replace it with a spare and get RICH-1 back in action "quickly".

How to support Tracker 1 is not yet decided; it may have to be supported from RICH-1.

## 4 External constraints

RICH-1 is placed inside the machine tunnel, so the space around it is limited: upstream by Tracker 1 and the Vertex Detector, downstream by Tracker 2 and the magnetic field shield plate and sideways by the tunnel walls.

Stray magnetic field in the region of RICH-1 is expected to be approximately 3mT (mostly in the y-direction). Given the considerable uncertainty in this figure, we plan to be able to work in a field twice as strong.

The radiation levels in the region of RICH-1 vary from 1 MRad/year near the beam-pipe to 1 kRad/year at a radius of 1m from the beam-pipe.

The machine tunnel is not clean; components sensitive to dirt will need adequate protection and somehow we must be immune to electrical and acoustic interference.

## 5 Description of the layout

Figure 1 shows a schematic view of RICH-1.

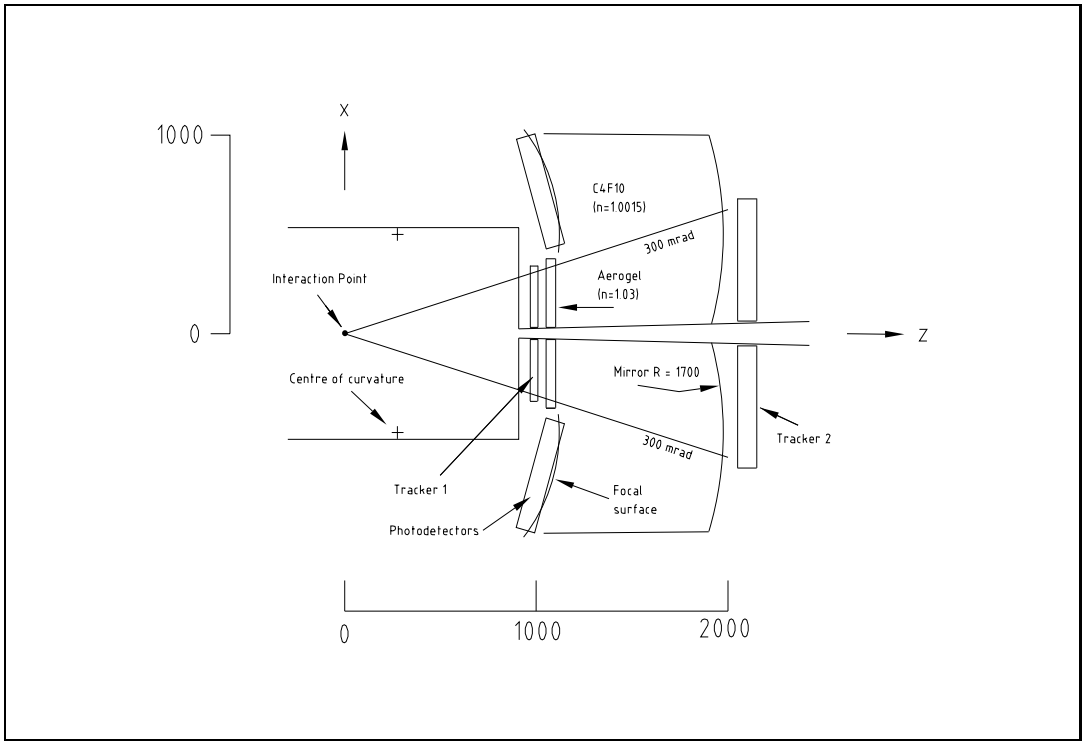


Figure 1: Layout of the RICH-1 detector (seen from above).

The Čerenkov light is focussed by a single mirror, whose radius is approximately equal to the distance from the interaction point, onto the focal surface. The mirror is divided into quadrants, each of which is tilted about the y-axis to bring the useful parts of the focal surface out of the acceptance and also about the x-axis to separate them at the horizontal median plane.

The photodetectors are grouped into 4 quadrants. Their photocathodes are placed on planes, each tilted to the best approximation to the useful parts of the focal surface.

There are two Čerenkov radiators: 50mm of Aerogel with index of refraction ≈1.03 and ≈800mm of $C_4F_{10}$ with index of refraction 1.0015.

## 6 Optimisation of the parameters

The choice of the mirror radius R and the tilt angles depends greatly on the crowded region where light emitted by wide-angle tracks in the Aerogel passes near reflected light emitted by small-angle tracks in the gas (see figure 2).

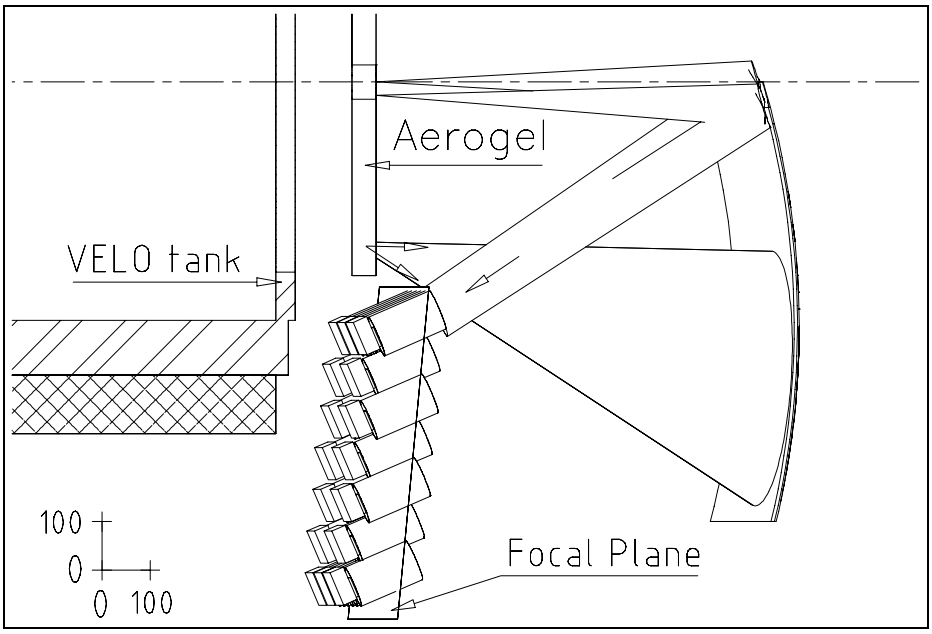


Figure 2: Plan view of the region between Aerogel and HPDs.

The intersections of photons, emitted by a sample of tracks filling one quarter of the acceptance, with the focal plane are shown in figure 3 along with the sensitive areas of the HPDs.

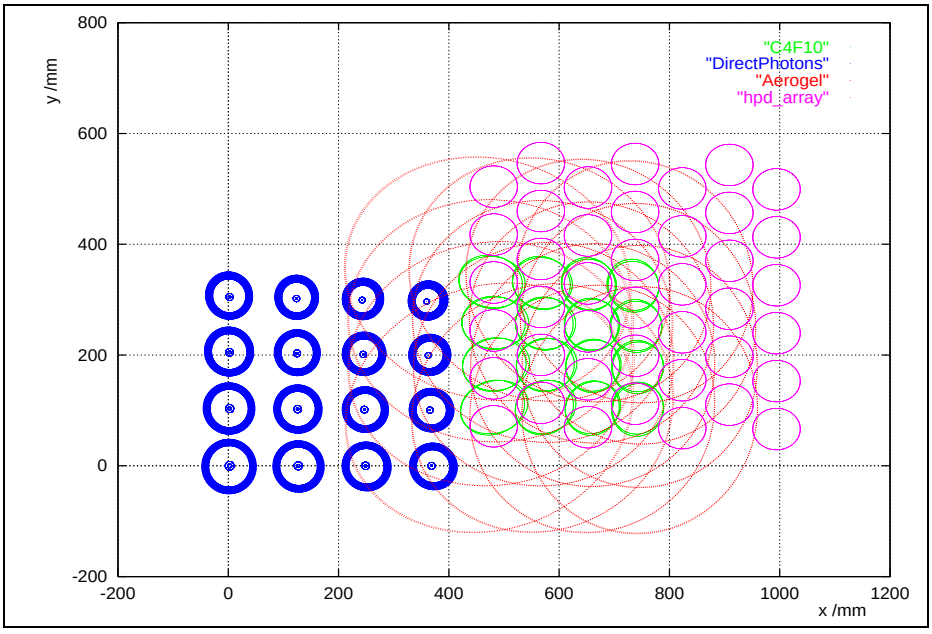


Figure 3: Positions of direct and reflected photons on the focal plane.

Mechanical details are also relevant, so the optimisation has been iterative. First we guess a suitable radius of curvature and tilt for the mirror. Then we find the plane which best approximates to the focal surface as follows. Sampling the acceptance uniformly (so that rare

tracks are not sacrificed to the mass), we consider the postions of photons as they cross an adjustable plane and minimise the variance between photons emitted from the upstream end of the track and those emitted from the downstream end. If the ring-image for any track clashes with the mechanics, we guess again. The result is:

- Centre-of-curvature at (±500, ±110, 275)mm,
  (corresponds to tilt = ≈300mrad horizontal, ≈65mrad vertical)
- R = 1700mm. The centre-of-curvature is no longer at z=0, but the effect of this is accounted for when the Čerenkov angles are calculated to find the emission-point error.

The performance is degraded somewhat compared to the Technical Proposal [1]. The increased tilt degrades the emission-point error; for light emitted in the gas, it increases from 0.54mrad to 0.76mrad. The shorter focal length increases the error due to the pixel size; from 0.72mrad to 0.80mrad. The table shows the various contributions to the total error.

| | | TP | | Current design | |
|---|---|---|---|---|---|
| | | $C_4F_{10}$ | Aerogel | $C_4F_{10}$ | Aerogel |
| $\sigma_\theta^{\text{emission}}$ | [mrad] | 0.54 | 0.36 | 0.76 | 0.41 |
| $\sigma_\theta^{\text{chromatic}}$ | [mrad] | 0.54 | 1.21 | 0.54 | 1.21 |
| $\sigma_\theta^{\text{pixel}}$ | [mrad] | 0.72 | 0.72 | 0.80 | 0.80 |
| $\sigma_\theta^{\text{total}}$ | [mrad] | 1.10 | 1.45 | 1.23 | 1.51 |

## 7 Preliminary ideas for the implementation

We assume that Trackers 1 and 2 do not extend outside "their territory" ($z < 1030, z > 2050$mm), and that Tracker 1 is limited to $|x| \leq 400$mm. We have made two further assumptions to simplify the design process. The first is that we can use a **single** support frame surrounding the beam-pipe permanently, rather than one that can be divided into two pieces and withdrawn on each side. The second is that a window is allowed between the photodetectors and the gas radiator so that the HPDs can be outside the gas.

Figure 4 shows how the main components of RICH-1 are arranged.

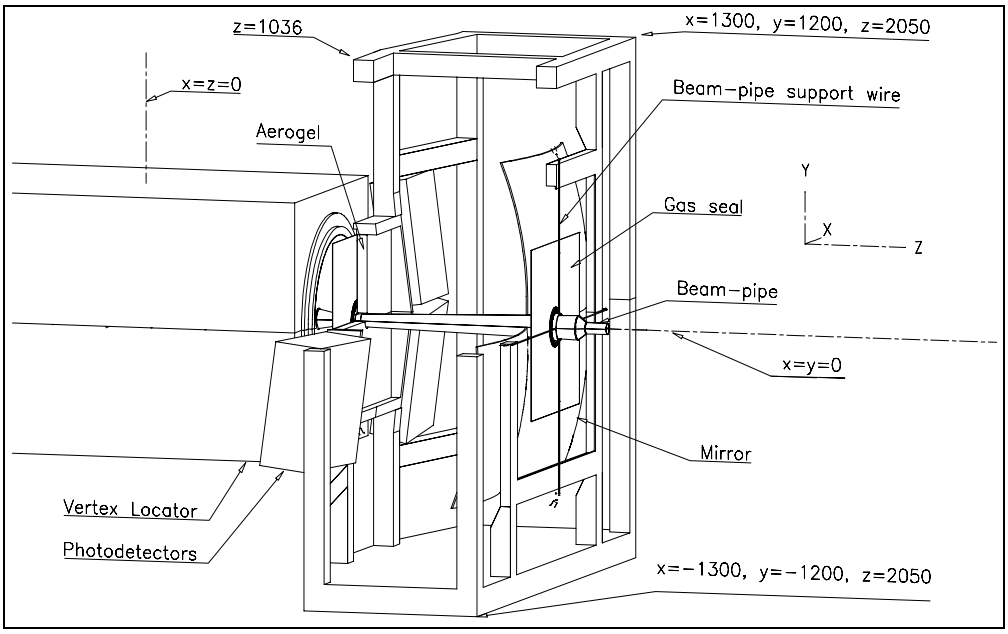


Figure 4: General arrangement of (three quarters of) RICH-1.

### 7.1 Support frame

Many particles emit light into both sides of the counter, so that the central plane, x=0, must be transparent. A single framework makes this automatic and also eases the problem of making the counter gas-tight. The beam-pipe needs supporting in any case; a separate support would presumably take more space.

A single frame has the following implications:

i) There can always be support for the beam-pipe; both during operation and during its installation.
ii) The beam-pipe has to be protected when we work inside RICH-1.
iii) Most RICH components (Aerogel, mirrors, photodetectors and windows) have to be removed when the beam-pipe is moved and probably when it is baked out too.
iv) The frame is intimately involved in the installation and removal of the beam-pipe.
v) There is no access to the beam-pipe without removing the gas.

The beam-pipe must be kept in position to $\approx \pm 0.1$mm in x and y by support wires with $\approx$100N tension each, those at +x, +y defining the position and those at -x, -y defining the tension. These will not constrain z; the axial force to do so will be exerted by a "fixed point" downstream of RICH-1 near the magnetic shield plate.

The mirrors will need similar precision of position to avoid clashing with the beam-pipe since the clearance will be kept to $\mathcal{O}(1\text{mm})$. In addition, their angle must be stable to $\approx$0.1mrad.

Welded stainless-steel box-section stiffened by plate will form the main frame. A rigid "floor" at y$\approx$-1.1m will allow convenient access to beam height and provide the base for a temporary "bench" just below the beam-pipe which will support protective shields for the

beam-pipe during access and equipment for installing the gas-seals.

RICH-1 will rest on 3 support points which will define the height to 0.1mm. During installation of the beam-pipe, the frame will be required to move approximately 2.5m in x and 0.1m in z. This movement could conveniently be made using air-skids [2] on a smooth base-plate fixed to the concrete floor. This base-plate could also incorporate the three slightly raised support points. The air-skids would help to keep the support-points clean, but would have to work without any flexible diaphragm between skid and support. The positions in x and z would be defined by dowels engaging with plates mounted on the frame. Fine adjustment of x and z would be made by moving the dowel plates and of y by jacking the air-skids. The dowels would need to be big enough to define x and z even with a gap as big as the range of adjustment in y and would need a sphere at one end to allow for rotation.

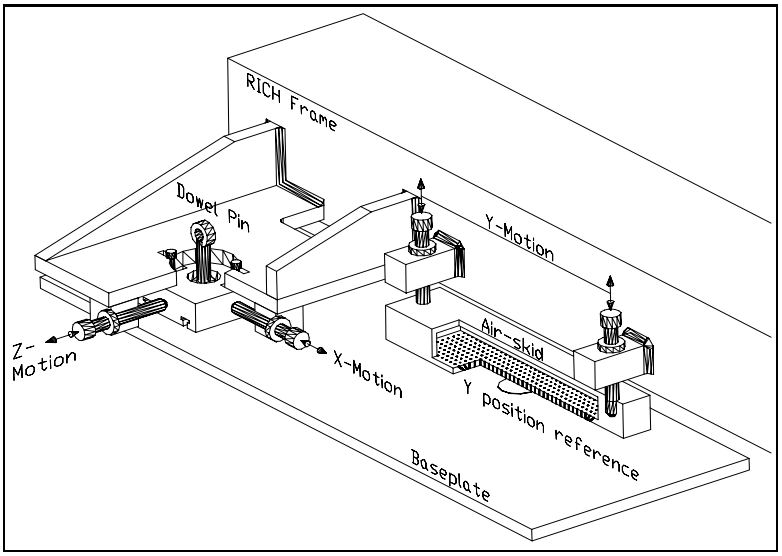


Figure 5: Section through one support of the RICH-1 frame.

The present concrete floor is at y=-2150, which is lower than we would prefer.

### 7.2 Photodetectors

Pixel HPDs ( figure 6 )

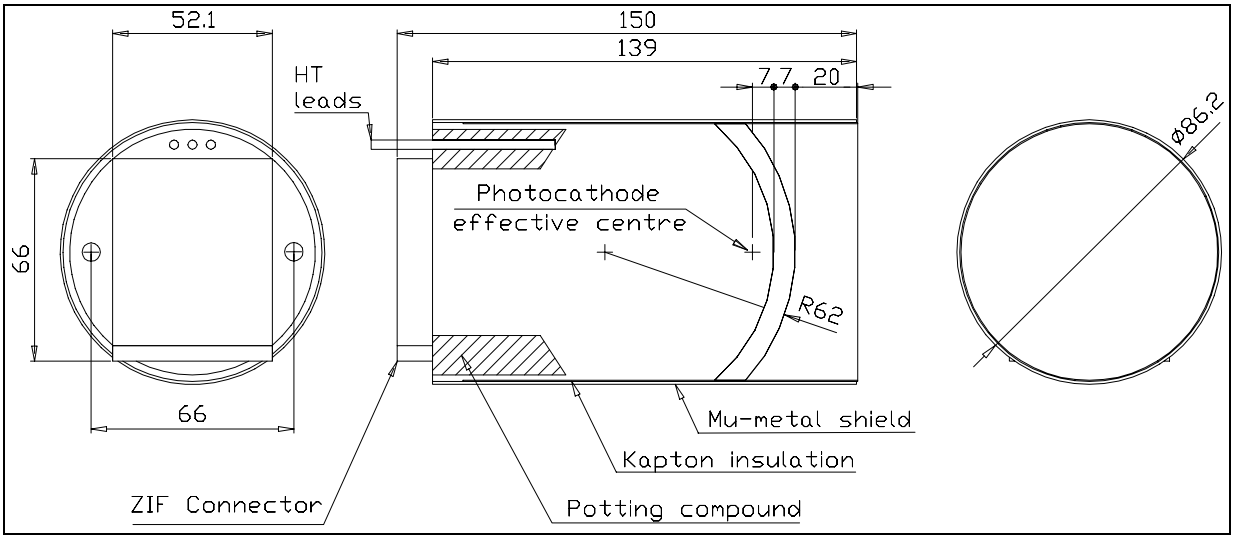


Figure 6: Pixel HPD with mu-metal shield.

are arranged in a hexagonal close-packed array at 87mm spacing with an electronics card serving each pair (figure 7).

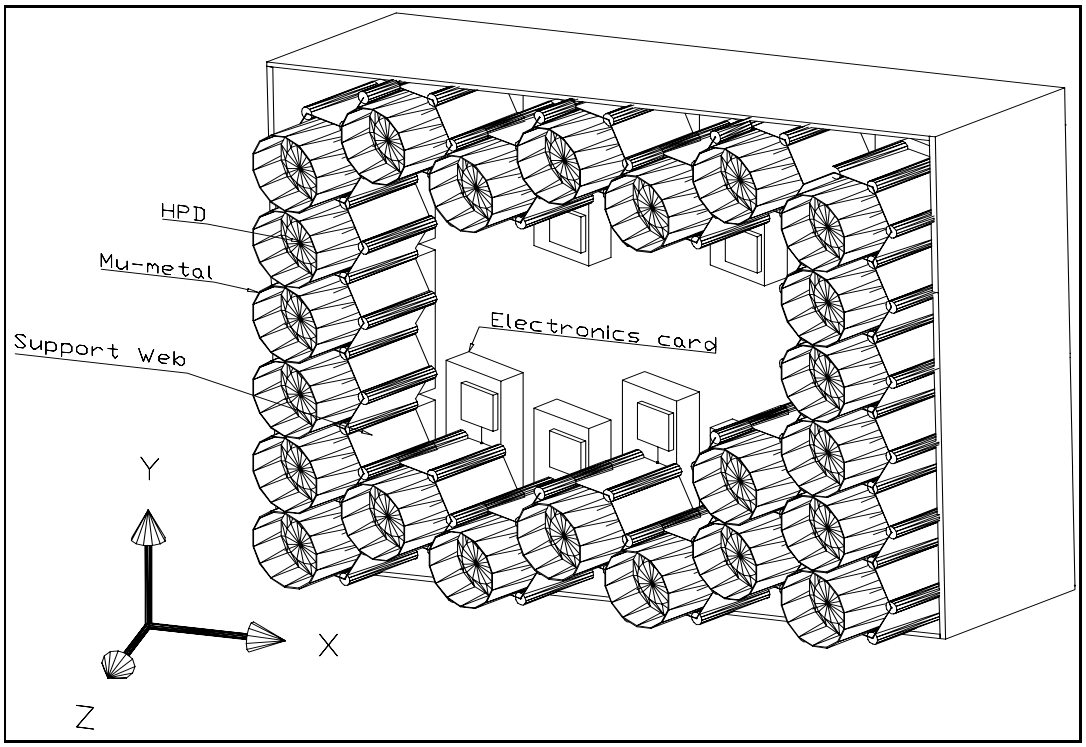


Figure 7: Part of the photodetector array for one quadrant.

Each HPD is shielded against up to 3mT [3] by a grounded cylinder of 0.9mm thick mu-metal extending 20mm beyond the photocathode window. The high-tension parts of the HPDs are insulated from the mu-metal by 2 layers of 125$\mu$m Kapton film. We assume that all electrical connections to the HPDs are made through the end opposite the photocathode.

Since the photocathode window is curved, we have chosen to locate the tubes so that a point 14mm behind the centre of the entrance window lies on the chosen focal plane.

The HPDs must point towards the incident light so that the mu-metal shields of a HPD and its neighbours cast minimal shadows on its photocathode. Their axes are therefore not normal to the plane tangent to the photocathodes, but rotated towards the beam by $\approx$ 500mrad horizontally and away from the beam by $\approx$ 125mrad vertically.

The mu-metal cylinders are located in a hexagonal web which puts a 0.5mm stainless-steel sheet between each cylinder. The stainless-steel sheets are glued in slots in aluminium rods at the corners of the hexagons. As the glue may interfere with grounding, we are looking into alternative methods of fabrication. The hexagonal web is built up with increasing offsets along the HPD axis for successive HPDs so that there is the correct angle between HPD axes and the plane tangent to the photocathodes. An aluminium frame surrounds the hexagonal web, providing the means to withdraw and replace the quadrant reproducibly.

Figure 8 shows the contributions to the gap between HPDs whose diameters are $83^{+0.2}_{-0.1}$mm.

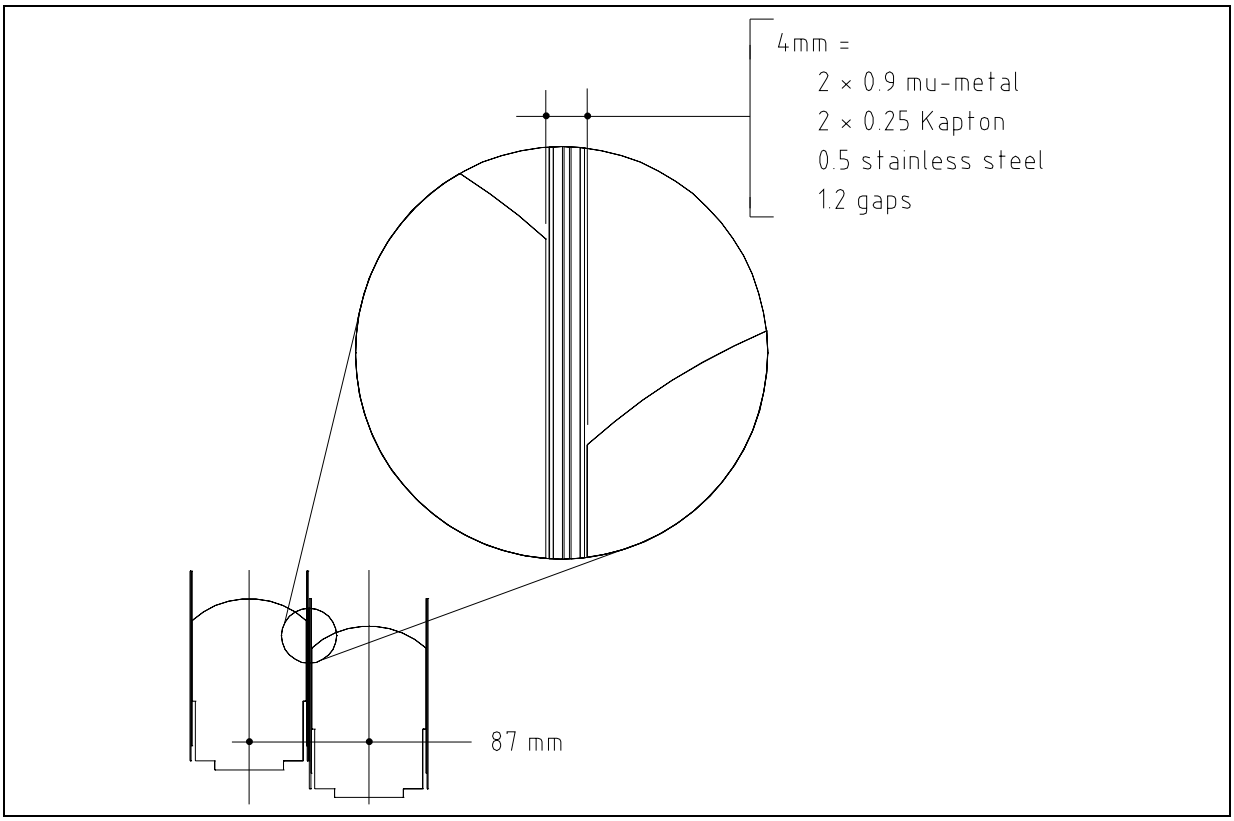


Figure 8: Detail of the region between two HPDs.

The HPDs are located radially by the hexagonal web to $\pm 1.2/\sqrt{12} = 0.35$mm on average. A black plastic moulding, screwed to the HPD and 3 pillars of the web, will locate them in z and provide some light-tighting.

Each photodetector quadrant will be maintained in an atmosphere of dry nitrogen to discourage electrical breakdown and the intrusion of helium.

### 7.3 Mirrors

Each quadrant is divided into 4 segments of 6mm glass supported at their centres. The support is designed to allow independent adjustment of each plane of movement from outside the RICH gas radiator volume.

Each quadrant is divided into equidistant segments as observed in the vertical and horizontal planes. This results in the mirror segments lying on a spherical surface with their edges defined by planes of constant x and constant y. The mirrors are quasi-rectangular in shape but with varying dimensions, ranging from the smallest dimension of $587 \times 584$ mm$^2$ (diagonal chord lengths) to that of the largest $612 \times 584$ mm$^2$, (see Figure 9.)

Figure 10 shows the support structure for each mirror. The support structure consists of a 3-legged spider and is made of a composite material. The legs radiate from a central (hollow) cylinder fixed to the mirror with an epoxy resin. This central position is the only place where the spider is affixed to the mirror. Incorporated at the end of the central support leg is a cone-like structure which rests on a ball mounting attached to the mirror mounting backplane. The height of each ball can be adjusted. At the end of each of the perpendicular legs is a V-shaped groove which engages an adjustment/alignment mechanism, Figure 11. Near the end of each leg is attached a spring under tension, which is also attached to the mirror mounting backplane. This ensures the adjustment/alignment mechanism remains permanently engaged in the V-shaped groove with no tension being applied to the mirror but only to the support structure.

The alignment mechanism, Figure 11, consists of an anti-backlash worm gear that drives an eccentric wheel that travels up or down the groove on the spider. As each of these mechanisms is mounted in a perpendicular configuration it allows independent alignment in the horizontal and vertical planes. To ensure the necessary aligment accuracy, it is envisaged to have a $50:1$ gearing at this stage. The drive shafts for the worm gears run parallel to the plane containing the mirror, to the outside of the RICH vessel.

The spiders are arranged on the back of the 4 mirrors in a way which minimises the amount of material from the supports that falls in the acceptance of the LHCb detector. The proposed layout is shown in Figure 12.

### 7.4 Gas envelope

We do not try to work with constant gas pressure. In order to minimise the stress on the most fragile parts of the gas envelope, gas will be supplied at the local atmospheric pressure within a few hundred Pascals. The density of $C_4F_{10}$ implies that the pressure difference between bottom and top of a 2m high vessel is $\approx$160Pa (17mm water). Since the gas supply

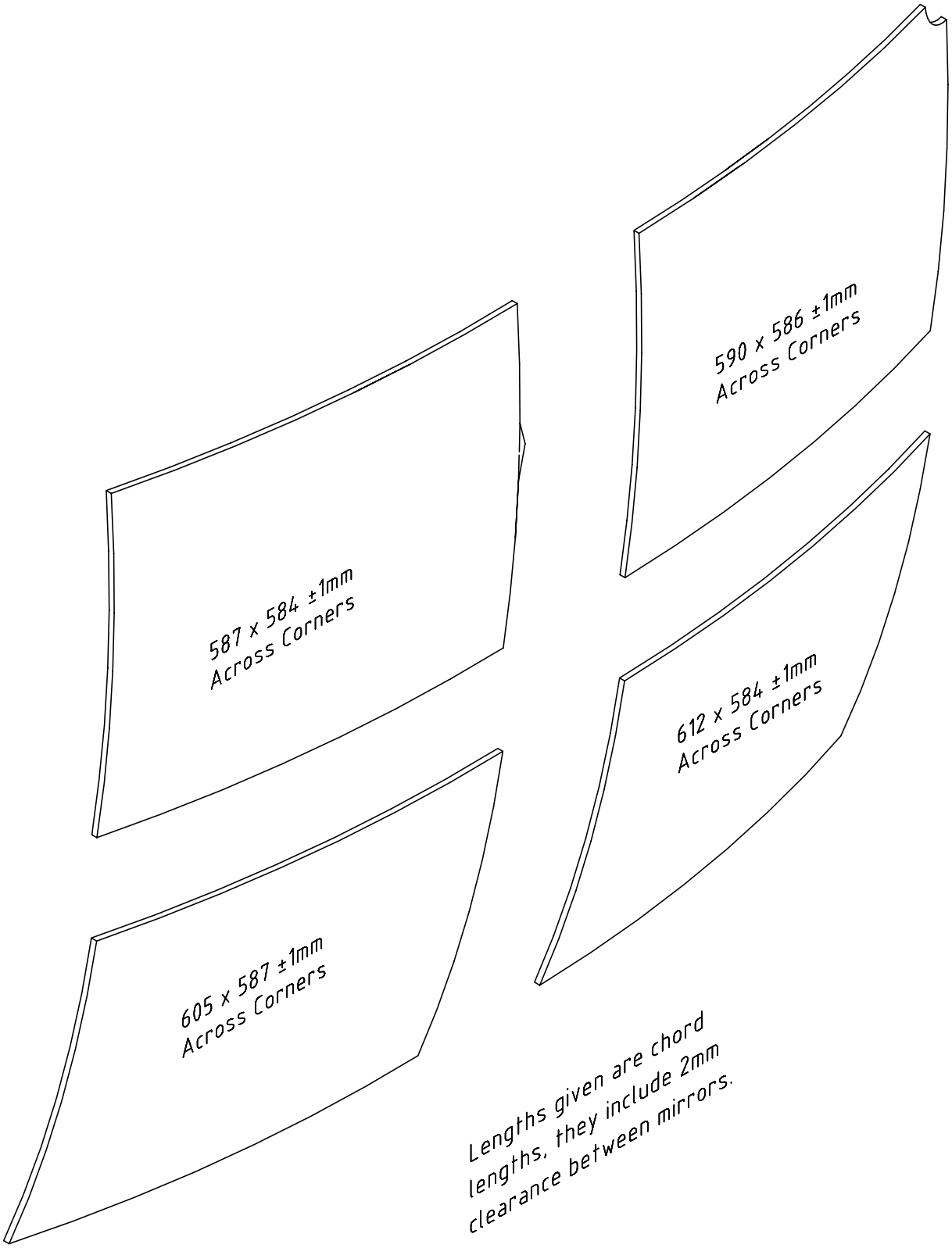


Figure 9: Dimensions of the 4 mirrors in a single quadrant. The mirror sizes are repeated in the other quadrants.

Figure 10: Rear view of one of the mirrors showing the mounting mechanism.

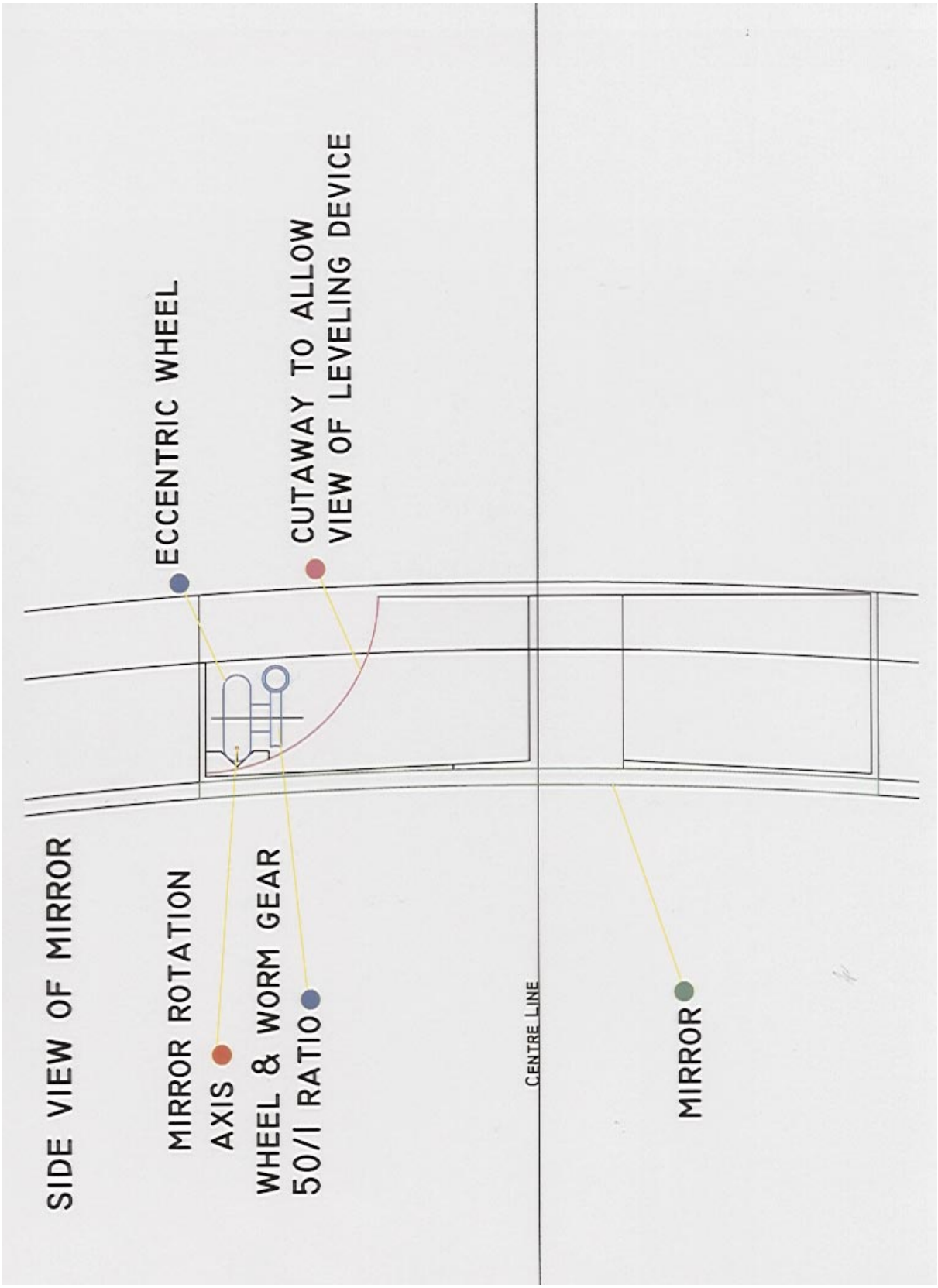


Figure 11: Side view of one of the mirrors showing the alignment mechanism.

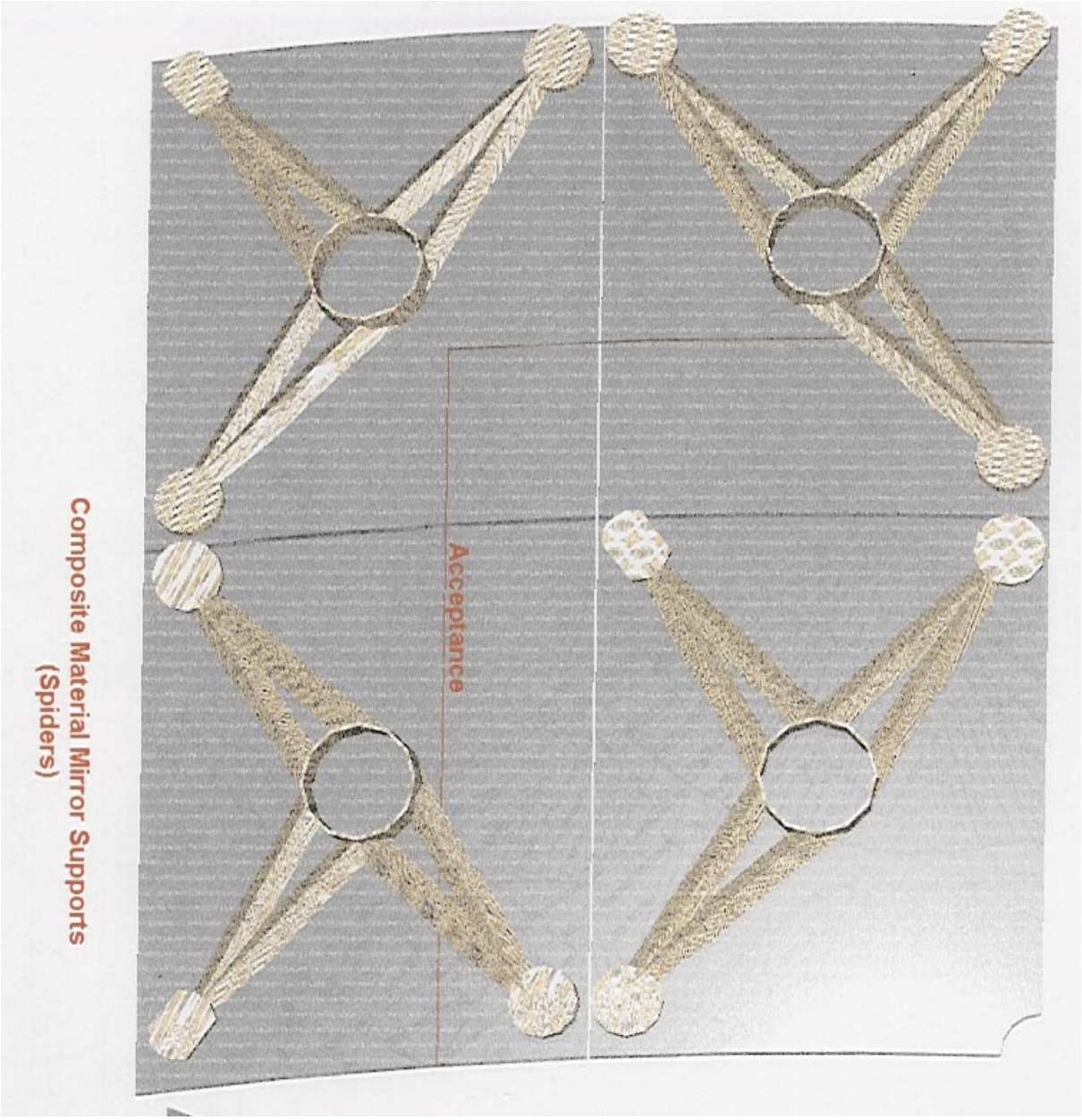


Figure 12: Rear view of one of the 4 mirrors in a quadrant showing the layout of the spiders in order to minimise the material within the experimental acceptance. The squarer padel represents the ball mounting.

will respond adequately to rapid changes in the atmospheric pressure, a local buffer volume is considered unnecessary.

To minimise the loss of acceptance at small angles, the beam-pipe is used as part of the gas envelope. If thermal insulation or absorber are needed, they will be added outside the beam-pipe; the materials used must be compatible with $C_4F_{10}$.

Within the acceptance of the spectrometer, the gas seals must be thin. They consist of 3 layers of 50$\mu$m Kapton glued to flanges on the beam-pipe and extending to a radius of approximately 200mm [4]. They are shown in figure 13.

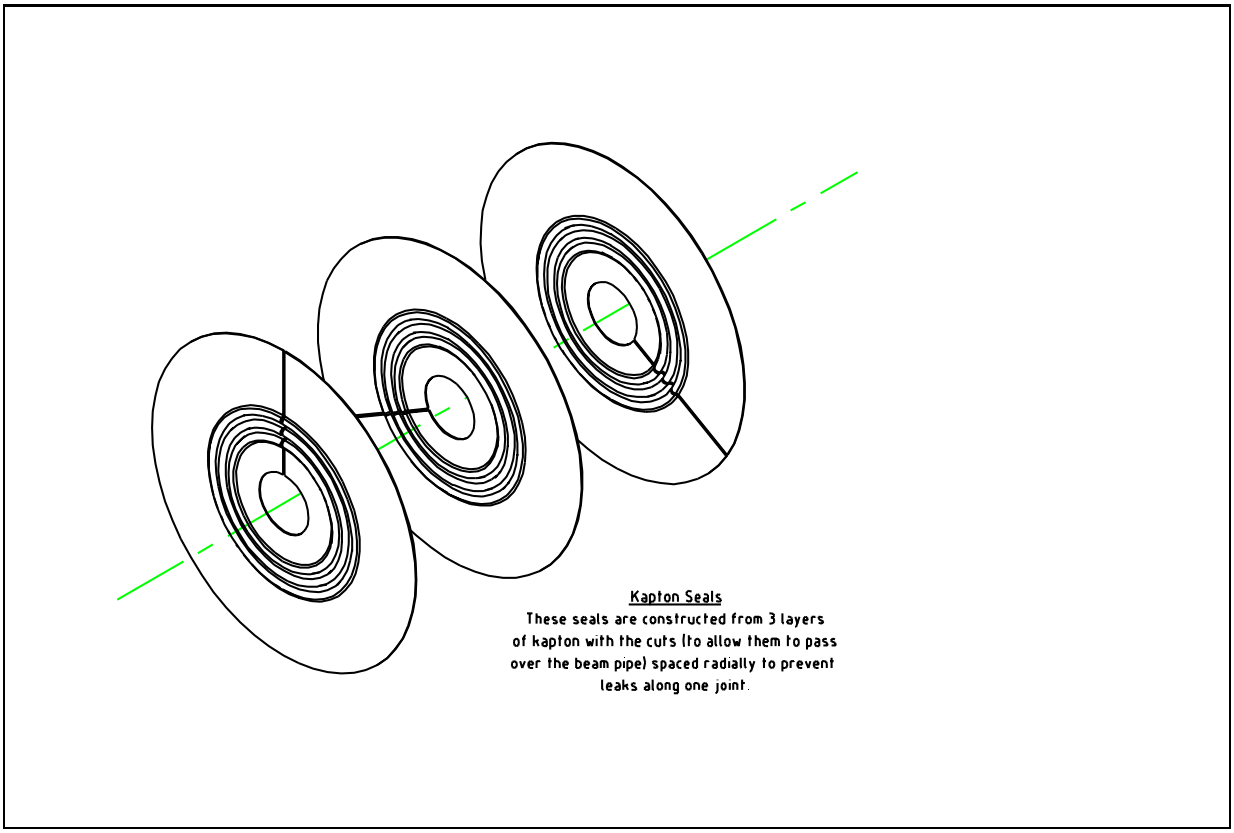


Figure 13: Kapton sealing foils.

The beam-pipe must not be stressssed too much, so undulations are moulded in which limit this. The three layers have to be cut radially, passed over the beam-pipe and then bonded together in place before being glued to the flange. Beyond 200mm, the Kapton foils will be glued to thin carbon-fibre sheets which seal the rest of the acceptance. The seals must also be light-tight; we are considering black Kapton (if mouldable) and aluminium coating.

In front of the photodetectors, the gas is sealed by windows of 6mm [1)] fused-silica. These are glued to thin aluminium frames which bolt to the main frame with inflatable seals.

Stainless-steel panels will be used elsewhere.

[1)] Such a thickness should support a pressure difference of 8000Pa with a safety factor of 4 [5].

### 7.5 Aerogel

The Aerogel radiator will be assembled from tiles at least $100 \times 100 \times 20$mm in size. There will be two halves or 4 quadrants housed in envelopes of $250\mu$m thick transparent plastic. A material with better radiation-tolerance than Mylar needs to be found for this.

### 7.6 Cabling

Cables and optical fibres about 90m long carry the signals and control levels between the photodetectors and electronics racks in the counting room. Those associated with each column of HPDs will be grouped together and led away vertically to cable trays above and below RICH-1. In order to have a minimum of disconnections when each quadrant of HPDs is moved sideways for servicing, the cable trays will pivot to allow the cables to follow.

## 8 Installation and alignment

The positions of the RICH-1 components which need to be known for the reconstruction are those of the centres-of curvature of each mirror quadrant, the centre of the photocathode of each HPD, the directions of the axis of each HPD and the positions of the Aerogel tiles. We expect to install RICH-1 with each of these known to $\pm 0.5$mm in x,y and $\pm 2$mm in z, using the same coordinate system as used by the Tracking. The centre of the frame will lie on the z-axis and it will be generously provided with survey marks.

### 8.1 Of the beampipe

This delicate component has to be supported at all times; it will be delivered with some sort of scaffolding as indicated in figure 14.

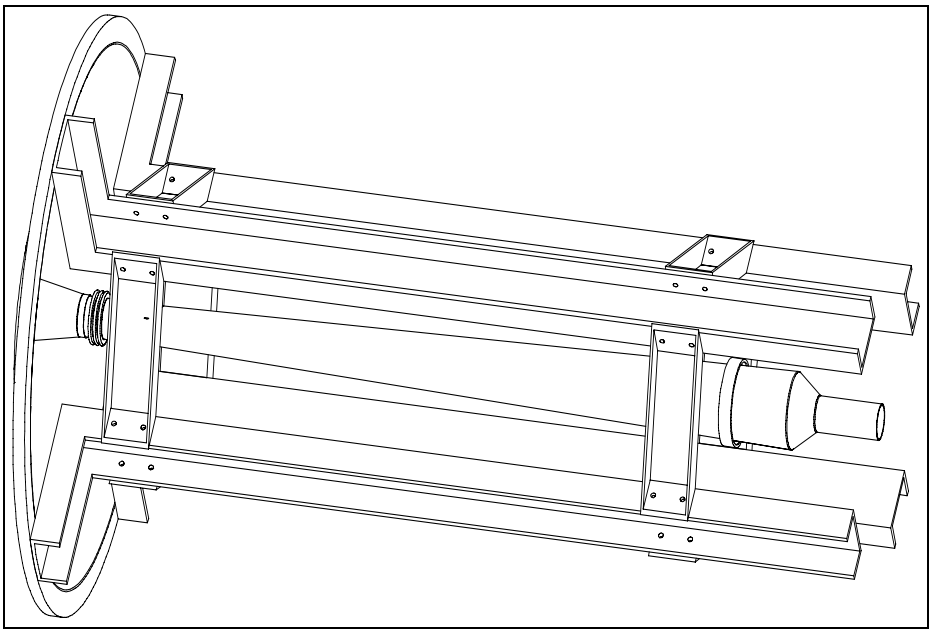

Figure 14: Beam-pipe with its support scaffolding.

Here we just sketch the installation procedure, which is described more fully in [6]. Together with its scaffolding, the beam-pipe will be inserted in the RICH-1 frame, which will have been moved ≈2.5m towards -x and ≈100mm downstream. (See figure 15).

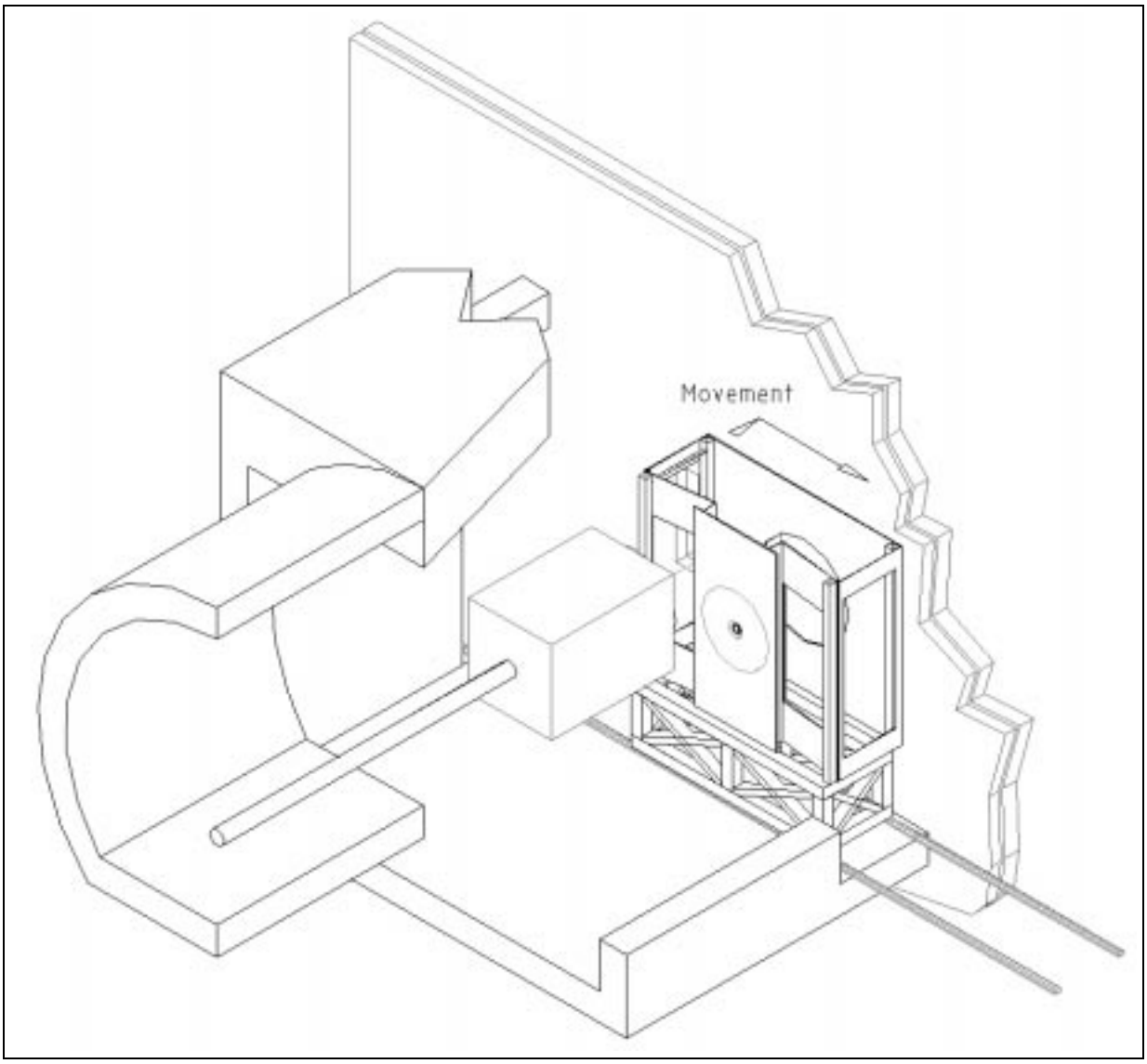


Figure 15: The RICH-1 frame and beam-pipe withdrawn from the beam-line.

Then, after moving the frame to its final position, the support of the beam-pipe flange will be transferred to the vertex detector tank. This will require the beam-pipe and its scaffolding to move slightly within RICH-1 while still being supported by it. After transferring the support of the beam-pipe tube from the scaffolding to the support wires, the scaffolding will be dismantled. Since the beam-pipe protrudes downstream of RICH-1, Tracker 2 will have to be absent during this manoeuvre.

### 8.2 Of the mirrors

Each of the 4 segments in a quadrant has to be adjusted so that its centre-of-curvature lies at the position of the common centre-of-curvature for that quadrant. We expect to do this with two quadrants on each side withdrawn from the RICH-1 frame so that the centres-of-curvature are accessible. The positions of the centres-of-curvature relative to the mirror support will then be found; these must be preserved when the mirrors are moved inside. Finally, the mirror supports will be surveyed in the working position.

During setting-up, there will be a time when the mirrors have been moved into the RICH vessel after being aligned outside and we have not yet got confidence in whatever test-patterns are available. We can at least simulate Čerenkov light using a compact arrangement of light-source,lens and conical prism [7]. The light generated can be shone on the boundary of mirror segments to verify their relative alignment.

### 8.3 Of the photodetectors

Each HPD with its insulation and mu-metal will be made to work on the bench so that it can just be "plugged in" to the HPD array.

Given the distortion in the electron optics arising from the magnetic field, calibration will be needed.

There are at least two problems. The problem local to each HPD is where the centre of the photocathode maps on the pixel array and what are the distortions in mapping the rest of the photocathode. This can presumably be dealt with using an illuminated mask on each HPD. Then there is the problem of locating the centre of each photocathode in the (x,y,z) coordinate system; presumably by surveying the masks. However, when a HPD is replaced, we do not want to have to resurvey. The hexagonal web will locate each HPD mechanically to $\approx \pm 0.4$mm but is desirable to improve on this. One possibility is to project light beams parallel to each HPD axis onto the photocathodes and read out their positions via the DAQ. Each light beam should be large enough that illuminated neighbouring pixels can be used to interpolate its position more precisely than a single pixel would allow and could be produced by an array of LEDs and a mask as shown in figure 16. Both array and mask would be located into pre-surveyed positions. We assume that the position in z and the direction of the HPD axes will not need checking because defined well enough by the mechanics.

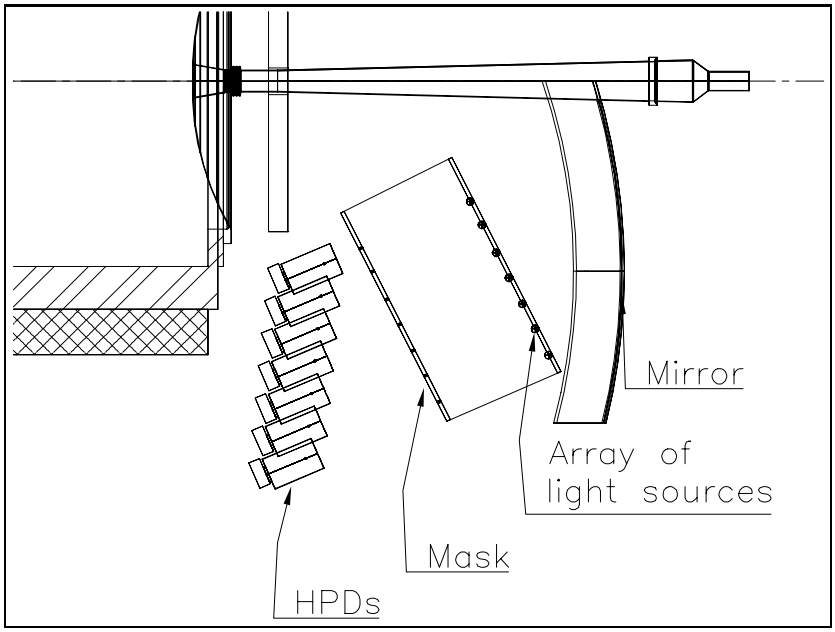


Figure 16: Gadget to check the alignment of the HPDs.

## 9 Operations

### 9.1 What might we have to do ?

Here we just mention some obvious tasks; the list is bound to get longer.

- Mend light leaks.
- Mend gas leaks. ( But how to find them ? )
- Keep the gas pure. ( No problem if no leaks, done upstairs. )
- Adjust the mirrors. ( Anytime we find them badly mis-aligned – ie. $> \mathcal{O}(1\text{mrad})$. )
- Bake out the beam-pipe. ( $\Rightarrow$ emptying RICH. )
- Replace photodetectors. ( $\Rightarrow$ withdrawing a quadrant to do so. )
- Replace some Aerogel. ( $\Rightarrow$ access inside RICH $\Rightarrow$ removing the gas. )
- Replace the beam-pipe.

## 10 Monitoring

### 10.1 Alignment

During running, this will be most conveniently done using tracks. Reference [8] suggests that reconstructing a few hundred events will allow the offsets of the mirror segments to be measured accurately enough provided that the initial alignment is good to a few mrad.

During shut-downs, we expect to project test-patterns onto the HPDs via the mirrors. This will give a quick check of possible changes. Some possibilities are described in [9].

### 10.2 Refractive index

The best information will be obtained by using tracks. An additional check could be to monitor the speed of sound in the $C_4F_{10}$, calibrating this by measuring the refractive index using interferometry.

### 10.3 Photocathode sensitivity.

During running, tracks will allow this to be monitored. If changes are observed, a measurement of the frequency-dependence using a deuterium lamp and monochromator could help diagnosis. Čerenkov light from betas in fused-silica might allow an absolute measurement of sensitivity without beam.

## 11 Discussion

What is missing ?

– A complete specification for the gas-system, including its response to rapid changes in atmospheric pressure and our requirements for emptying and filling.
– A complete solution to the light-tighting problem:
  at the HPDs.
  at the gas seals.
  outside the groups of HPDs.
– A solution to the problem of keeping the HPDs in an atmosphere of dry nitrogen.
– Calculations to predict the deformations of the frame and mirror supports.
– A scheme for finding leaks and an estimate of the tolerable leak rate.

We list here some obvious weaknesses of the present design.

– A 7.7% loss of light in the fused-silica window.
– High-momentum tracks have worse resolution than the TP. (1.10 → 1.23mrad.)
– Identifying low-momentum tracks near the beam requires reconstructing the Čerenkov angle using light emitted by the Aerogel collected in all four quadrants.
– The optimisation was done for uniformly-distributed tracks; it would be possible to readjust the photodetector positions somewhat to improve the resolution for real data (or a realistic simulation).

Which features could be better or just simpler ?

– The crowded region between the Aerogel and the HPDs will be looked at further and may benefit from an increase in the focal length.
– An alternative way of fabricating the HPD support could help the light-tighting as well as making it simpler and more precise.

If the MAPMT option for the photodetectors has to be taken up, it will affect the mechanics; mainly by making the design easier. The local electronics cards would be bigger. Accomodating these implies either overlapping them with consequent inconvenience when working on them or the MAPMTs, or packing them behind the MAPMTs and sacrificing the possibility of increasing the focal length and reducing the tilt of the mirrors. With a suitable design of dynode chain, there would not be significantly more heat ($\mathcal{O}$(100W)/quadrant) to be removed. The cabling would be similar to that for the HPDs. The MAPMTs use focussing lenses to improve their sensitive area. Combining these with the gas window is an attractive possibility.

## 12 Safety

### 12.1 Electrical

Pixel HPDs do not draw significant current, so the high-voltage supplies can be limited to give currents which are "safe"; of order 0.1mA for a column of twelve HPDs. The supplies will be behind the shield-wall so that the connecting cables of ≈100m will store up to 2.5J each. This is not considered dangerous; ref [10] accepts stored energies of up to 10J.

### 12.2 Mechanical

The fused-silica windows will have to be protected by a safety valve in the gas system releasing at 500Pa and proved at a pressure of 3500Pa [11].

### 12.3 Gas

$C_4F_{10}$ is asphyxiating and heavy, nitrogen is asphyxiating. In the enclosed space around RICH-1, it will be necessary to have monitors for lack of oxygen controlling an extraction system removing gas near the floor.

## 13 Acknowledgements

We thank J. Maxwell for useful discussions on optical matters and
M. Dowman for preparing a prototype fused-silica window.

# A Appendix; RICH-1 Parameters

## A.1 Materials

| | $X_0$ | |
|---|---|---|
| Entrance window | 0.06% | 150$\mu$m Kapton |
| Aerogel | 3.3% | |
| $C_4F_{10}$ | 2.6% | |
| Mirror | 4.8% | 6mm glass |
| Mirror support | <2.6% | averaged over the aperture |
| Exit window | 0.06%<br><1.0% | 150$\mu$m Kapton<br>2mm carbon fibre |
| Total | <14.4% | |

## A.2 Mirrors

Radius of curvature = 1700mm,

Centres of curvature at (±500, ±110, 275)mm,

Outside edges at x = ±900mm, y = ±750mm.

Focal planes pass through ( 0, 0, 1256)mm with
direction cosines = ( ±0.094072, ±0.1029146, 0.990232).

## A.3 Photodetectors

The HPD axes have direction cosines ( ±0.394732, ±0.094139, 0.913961).

The centres of the outsides of the HPD photocathode windows lie at

| HPD column | x | y | z |
|---|---|---|---|
| 1 | ±474.47 | ±71.32 | 1216.0 |
| | ±474.47 | ±157.86 | 1207.1 |
| | ±474.47 | ±244.40 | 1198.2 |
| | ±474.47 | ±330.94 | 1189.2 |
| | ±474.47 | ±417.49 | 1180.3 |
| | ±474.47 | ±504.03 | 1171.4 |
| 2 | ±559.95 | ±113.76 | 1203.5 |
| | ±559.95 | ±200.20 | 1194.6 |
| | ±559.95 | ±286.85 | 1185.7 |
| | ±559.95 | ±373.39 | 1176.8 |
| | ±559.95 | ±459.93 | 1167.8 |
| | ±559.95 | ±546.47 | 1171.4 |
| 3 | ±645.42 | ±69.66 | 1199.9 |
| | ±645.42 | ±156.20 | 1191.0 |
| | ±645.42 | ±242.75 | 1182.1 |
| | ±645.42 | ±329.29 | 1173.2 |
| | ±645.42 | ±415.83 | 1164.3 |
| | ±645.42 | ±502.37 | 1155.3 |
| 4 | ±730.89 | ±112.11 | 1187.4 |
| | ±730.89 | ±198.65 | 1178.5 |
| | ±730.89 | ±285.19 | 1169.6 |
| | ±730.89 | ±371.73 | 1160.7 |
| | ±730.89 | ±458.27 | 1151.8 |
| | ±730.89 | ±544.82 | 1142.9 |
| 5 | ±816.37 | ±68.01 | 1183.8 |
| | ±816.37 | ±154.55 | 1174.9 |
| | ±816.37 | ±241.09 | 1166.0 |
| | ±816.37 | ±327.63 | 1157.1 |
| | ±816.37 | ±414.18 | 1148.2 |
| | ±816.37 | ±500.72 | 1139.3 |
| 6 | ±901.84 | ±110.45 | 1171.4 |
| | ±901.84 | ±196.99 | 1162.4 |
| | ±901.84 | ±283.54 | 1153.5 |
| | ±901.84 | ±370.08 | 1144.6 |
| | ±901.84 | ±456.62 | 1135.7 |
| | ±901.84 | ±543.16 | 1126.8 |
| 7 | ±987.31 | ±66.35 | 1167.8 |
| | ±987.31 | ±152.89 | 1158.9 |
| | ±987.31 | ±239.44 | 1150.0 |
| | ±987.31 | ±325.98 | 1141.0 |
| | ±987.31 | ±412.52 | 1132.1 |
| | ±987.31 | ±499.06 | 1123.2 |

**References**


[1] LHCb technical Proposal CERN/LHCC 98-4
[2] Airfloat/HSI Systems Inc. (www.airfloat.com) sell skids which support 10T/m$^2$
[3] T.Gys and D.Piedigrossi, LHCb 2000-069 RICH.
[4] J.A.Lidbury et al. In preparation.
[5] Roark and Young, Formulas for stress and strain (5th ed.) pp 386, 410. We assume a yield stress of 50MPa (W.Englisch, Heraeus unpublished).
[6] G.J.Barber et al. LHCb 2000-078 RICH.
[7] D.M.Binnie, Private communication.
[8] F.Filthaut, Report to the RICH group 19/3/99, http://lhcb.cern.ch/rich/postscript/filthaut_190399.ps
[9] C.d'Ambrosio et al. LHCb 2000-080 RICH
[10] CERN Safety Instruction IS-28 cern.web.cern.ch/CERN/Divisions/TIS/safdoc/IS/is28/is28_en.html
[11] CERN Safety Instruction IS-34 cern.web.cern.ch/CERN/Divisions/TIS/safdoc/IS/is34/is34_en.html